Received: 19 July 2024 | Revised: 9 September 2024 | Accepted: 22 October 2024

DOI: 10.1002/dad2.70040

Alzheimer's & Dementia
Diagnosis, Assessment & Disease Monitoring

RESEARCH ARTICLE

Elevated tau in the piriform cortex in Alzheimer's but not Parkinson's disease using PET-MR

Hossein Moein Taghavi[1] | **Mahta Karimpoor**[1] | **Eric K. van Staalduinen**[1] | **Christina B. Young**[2] | **Marios Georgiadis**[1] | **Samantha Leventis**[1] | **Mackenzie Carlson**[2] | **America Romero**[2] | **Alexandra Trelle**[2] | **Hillary Vossler**[2] | **Maya Yutsis**[2] | **Jarrett Rosenberg**[1] | **Guido A. Davidzon**[1] | **Greg Zaharchuk**[1] | **Kathleen Poston**[2] | **Anthony D. Wagner**[3,4] | **Victor W. Henderson**[2,5] | **Elizabeth Mormino**[2,3] | **Michael Zeineh**[1]

[1]Department of Radiology, Stanford University School of Medicine, Stanford, California, USA

[2]Department of Neurology and Neurological Sciences, Stanford University School of Medicine, Stanford, California, USA

[3]Wu Tsai Neurosciences Institute, Stanford University, Stanford, California, USA

[4]Department of Psychology, Stanford University, Stanford, California, USA

[5]Department of Epidemiology and Population Health, Stanford University, Stanford, California, USA

Correspondence
Michael Zeineh, Department of Radiology, Stanford University School of Medicine, Lucas Center for Imaging, Rm. P271, 1201 Welch Rd, Stanford, CA 94305, USA.
Email: mzeineh@stanford.edu

Funding information
National Institutes of Health, Grant/Award Numbers: P30AG066515, P50AG047366, R21AG058859, R01AG048076, R01AG074339, R01AG061120, K99AG071837, R01NS115114; Alzheimer's Association, Grant/Award Number: ARFD-21-849349; Stanford Wu Tsai Neurosciences Institute; Stanford Precision Health and Integrated Diagnostics (PHIND) Center; Good Planet Foundation

Abstract

INTRODUCTION: Olfactory dysfunction can be an early sign of Alzheimer's disease (AD). We used tau positron emission tomography-magnetic resonance (PET-MR) to analyze a key region of the olfactory circuit, the piriform cortex, in comparison to the adjacent medial temporal lobe.

METHODS: Using co-registered magnetic resonance imaging (MRI) and ^{18}F-PI-2620 tau PET-MR scans in 94 older adults, we computed tau uptake in the piriform-periamygdaloid cortex, amygdala, entorhinal-perirhinal cortices, and hippocampus.

RESULTS: We found an ordinal cross-sectional increase in piriform cortex tau uptake with increasing disease severity (amyloid-negative controls, amyloid-positive controls, mild cognitive impairment [MCI] and AD), comparable to entorhinal-perirhinal cortex. Amyloid-positive controls showed significantly greater tau uptake than amyloid-negative controls. Negative correlations were present between memory performance and piriform uptake. Piriform uptake was not elevated in cognitively unimpaired Parkinson's disease.

DISCUSSION: Cross-sectionally, there is an early increase in tau uptake in the piriform cortex in AD but not in Parkinson's disease.

KEYWORDS
Alzheimer's, MRI, olfaction, PD, PET, PET-MR, piriform cortex, tau

Highlights

- Positron emission tomography–magnetic resonance (PET-MR) analysis of the piriform cortex sheds light on its role as a potential early region affected by neurodegenerative disorders underlying olfactory dysfunction.
- Uptake of tau tracer was elevated in the piriform cortex in Alzheimer's disease (AD) and mild cognitive impairment (MCI) but not in Parkinson's disease (PD).
- Memory performance was worse with greater piriform uptake.

1 | BACKGROUND

In Alzheimer's disease (AD), hyperphosphorylated tau (p-tau) exhibits a pathological progression in the brain as amnestic AD advances,[1] correlating with levels of cognitive decline.[2] Yet, challenges remain with early diagnosis and efficacious treatment.

The most common symptom associated with spectrum of AD is impaired memory formation and retrieval.[3] Memory circuitry typically involves the entorhinal cortex, the gateway of input to the hippocampus. Another common complaint in up to 90% of AD patients is an impaired sense of smell,[4–7] with diminished olfactory discrimination compared to patients with mild cognitive impairment (MCI), who in turn demonstrate degraded performance compared to healthy controls.[8] The human olfactory circuit intertwines with memory circuitry: olfactory receptors project through the cribriform plate to the olfactory bulb, and via the lateral olfactory tract to the piriform cortex, amygdala, and entorhinal cortex.[9] Notably, the piriform cortex is the primary cortical olfaction region in humans, and axons from the piriform cortex further project to other areas, including the periamygdaloid cortex,[10] which also receives neuronal signals downstream of the olfactory bulb.[11] Olfaction may be impacted in the early stages of not only AD[12–14] but also incipient Parkinson's disease (PD).[15–17] Senile plaques and tau are observed in the piriform cortex in postmortem studies of AD.[18] The noninvasive identification of tau deposition in that location could explain the early loss in odor discrimination in AD and/or PD and synergize with entorhinal cortical tau to affect memory function. Although olfaction is not measured in most AD studies, including the present study, it is still of interest to compare olfactory tau with memory circuitry and performance.

For the goal of translating tau assessment for in vivo imaging, new tau positron emission tomography (PET) tracer candidates, such as ^{18}F-PI-2620, display high affinity for hyperphosphorylated tau.[19,20] ^{18}F-PI-2620 has further shown reduced choroid plexus nonspecific uptake[21] and been translated efficaciously to in vivo human PET studies of the adjacent medial temporal lobe.[22] However, the piriform cortex has not been the primary subject of study in the tau PET literature. Furthermore, given the intersection of olfactory with entorhinal circuitry, piriform uptake may be of relevance to memory function, which, unlike olfactory function, is commonly measured in AD studies.

Our goal in this study is to measure and compare tau uptake in the piriform cortex, including the adjacent periamygdaloid cortex, across regions of the medial temporal lobe and across the stages of AD, in comparison to PD, correlating with available neurobehavioral testing encompassing memory performance. The piriform cortex and periamygdaloid cortex are immediately adjacent to one another and challenging to visualize as separate structures, so in this work we used multiple anatomic atlases to perform a rigorous segmentation of both their separate and combined boundaries, the latter of which we refer to as the piriform-periamygdaloid cortex (or piriform-PAC). We used ^{18}F-PI-2620 PET-MR to measure tau uptake in the piriform-PAC, entorhinal-perirhinal cortices, amygdala, and hippocampus cross-sectionally across AD, MCI, and amyloid-positive and negative healthy controls (HC) as well as PD.

2 | METHODS

2.1 | Cohort

We evaluated data from 162 participants from our ongoing ADRC (Alzheimer's Disease Research Center) and SAMS (Stanford Aging & Memory Study) studies. All participants gave written informed consent in accordance with Health Insurance Portability and Accountability Act (HIPAA) and the Stanford Institutional Review Board, which adheres to the ethical standards outlined in the 1964 Declaration of Helsinki and its subsequent amendments, with diversity, equity, and inclusion (DEI) considered by open enrollment without regard to race. Sixty-eight participants were excluded from our study due to not meeting inclusion criteria as outlined in Supplemental Methods.

Fifty-one of the 94 included participants were from the Stanford ADRC (10 AD, 8 MCI, 19 healthy controls [HCs], 14 PD), 31 were from SAMS (all HCs), 7 (all HCs) were dual enrolled in both SAMS and ADRC studies, and 5 AD participants were recruited separately through the memory clinic. Neuropsychological test battery data and clinical history and imaging from all participants were reviewed by a consensus panel of at least two neurologists, a neuropsychologist, and research staff in order to determine their respective diagnoses. PD was diagnosed using the UK Brain Bank criteria and required bradykinesia with muscle rigidity and/or rest tremor.[23] Please see Supplemental Methods for further details regarding enrollment.

2.2 | PET-MR scanning

Participants underwent a 90-min tau PET-MR (SIGNA, GE) using tau tracer ^{18}F-PI-2620 with a simultaneous co-registered sagittal T1-weighted three-dimensional (3D) IR-FSPGR (inversion-recovery fast spoiled gradient echo), as described previously.[22] Each participant also had an oblique coronal T2-weighted FSE (fast spin echo) perpendicular to the hippocampal long axis, either simultaneously or recently acquired (from an amyloid PET-MR within 2 years of the tau scan).

Time-of-flight (TOF) functionality was utilized following a 5–10 mCi intravenous injection of our tau PET radiotracer: ^{18}F-PI-2620 (Life Molecular Imaging, Inc.). Data were acquired at either 45–75 min or 60–90 min. We interpolated 60–90 min data to the 45–75 min timescale by using the intercepts and slopes of linear regressions that fit the signal intensity over time for each voxel using frame data, as has been described previously in Equation 1 from Pontecorvo et al.[24] During the PET acquisition, we acquired a sagittal T1-weighted IR-FSPGR (repetition time [TR] 7.6 ms, echo time [TE] 3.1 ms, flip angle [FA] 11, 1 × 1 × 1.2 mm resolution; 5 m 46 s scan time) and a coronal-oblique T2-weighted FSE (TR 14111 ms, TE 102.4 ms, FA 111, 0.43 × 0.43 × 1.9 mm resolution; 3 m 24 s scan time). Finally, to reconstruct the PET data set, we used a LAVA-Flex (liver-accelerated volume acquisition-Flex) MRI series in conjunction with a tissue atlas.

2.3 | Co-registration and hippocampal segmentation

The T1-weighted and T2-weighted FSE were co-registered using NiftyReg[25] and a symmetric affine transformation. Occasionally, the affine transformation produced distorted output, in which case a symmetric rigid transformation was successfully used. The T1-weighted scan was natively registered to the PET image, so combining transformations enabled full co-registration of the T1, T2 FSE, and PET images. Automatic Segmentation of Hippocampal Subfields (ASHS, 2017 version) was run utilizing the T1 and T2 FSE images to segment hippocampal subfields, including the entorhinal cortex, BA35 and 36 (here approximated as perirhinal cortex), CA fields, dentate gyrus (DG), and subiculum.

ASHS output was inspected for accuracy. All in the final cohort met quality control criteria for adequate segmentation and alignment. We combined ASHS subfields into two bilateral subregions: (1) entorhinal-perirhinal cortex (including BA35 and 36), and (2) whole hippocampus = CA1–4 + DG + subiculum.

2.4 | Manual segmentation of the piriform cortex

The piriform cortex is a C-shaped segment of cortex with frontal and temporal portions along opposing banks of the endorhinal sulcus (note that the endorhinal sulcus lies along the anteromedial aspect of the ambient cistern,[26] Figure 1D, and is distinct from both the rhinal sulcus and entorhinal cortex). We segmented three regions: frontal piriform cortex (PirF, on the superior bank), temporal piriform cortex (PirT, on the inferior bank), and periamygdaloid cortex (or PAC), which is contiguous along the posterior aspect of PirT and begins about 6 mm posterior to the limen insula. (Please see Supplemental Methods for further details regarding the manual segmentation procedures.) Our segmentation protocol was based on anatomic landmarks defined by histologic analysis[26–28] and is consistent with other imaging studies of the piriform cortex.[29–32] Using Insight toolkit (ITK)-SNAP,[33] we manually segmented each piriform region on coronal T1-weighted images with aid of co-registered T2-weighted FSE images (Figure S1), both in the same space visualized at 2 mm coronal slice thickness, with overlaid ASHS hippocampal subfield segmentations (Supplemental Methods).

RESEARCH IN CONTEXT

1. **Systematic review**: The authors initiated a comprehensive literature search via PubMed on the olfactory circuit, in particular, the piriform cortex, and how it is affected by Alzheimer's disease (AD)/mild cognitive impairment (MCI). Postmortem and functional magnetic resonance imaging (fMRI) studies have investigated the pathophysiology of the piriform cortex in AD, while only fluorodeoxyglucose–positron emission tomography (FDG-PET) has been utilized in this region. These publications laid the foundation for our current research.
2. **Interpretation**: When analyzing tau-PET uptake in the piriform cortex and comparing AD, MCI, and healthy controls (HCs), we found an ordinal increase in piriform tau uptake with increasing AD disease severity. In contradistinction, uptake was not elevated in Parkinson's disease.
3. **Future directions**: We show a tight association between piriform uptake and clinical AD memory metrics. Future work will include more detailed correlations with measures of olfactory function as well as blood/cerebrospinal fluid (CSF) AD biomarkers.

2.5 | Automatic segmentation of amygdala

In addition to automatic segmentation of hippocampal subfields, FreeSurfer's 7.2 amygdala segmentation module[34] was utilized. The added amygdala segmentation was ensured to be non-overlapping with the hippocampal subfield and piriform segmentations from previous steps by both automatically excluding overlapping voxels and manually excluding amygdala voxels going beyond the PirT.

2.6 | Quality checking the scans and manual segmentations

Automatic segmentations (amygdala and hippocampal subfields) were checked for consistency and overlap as described earlier, blinded

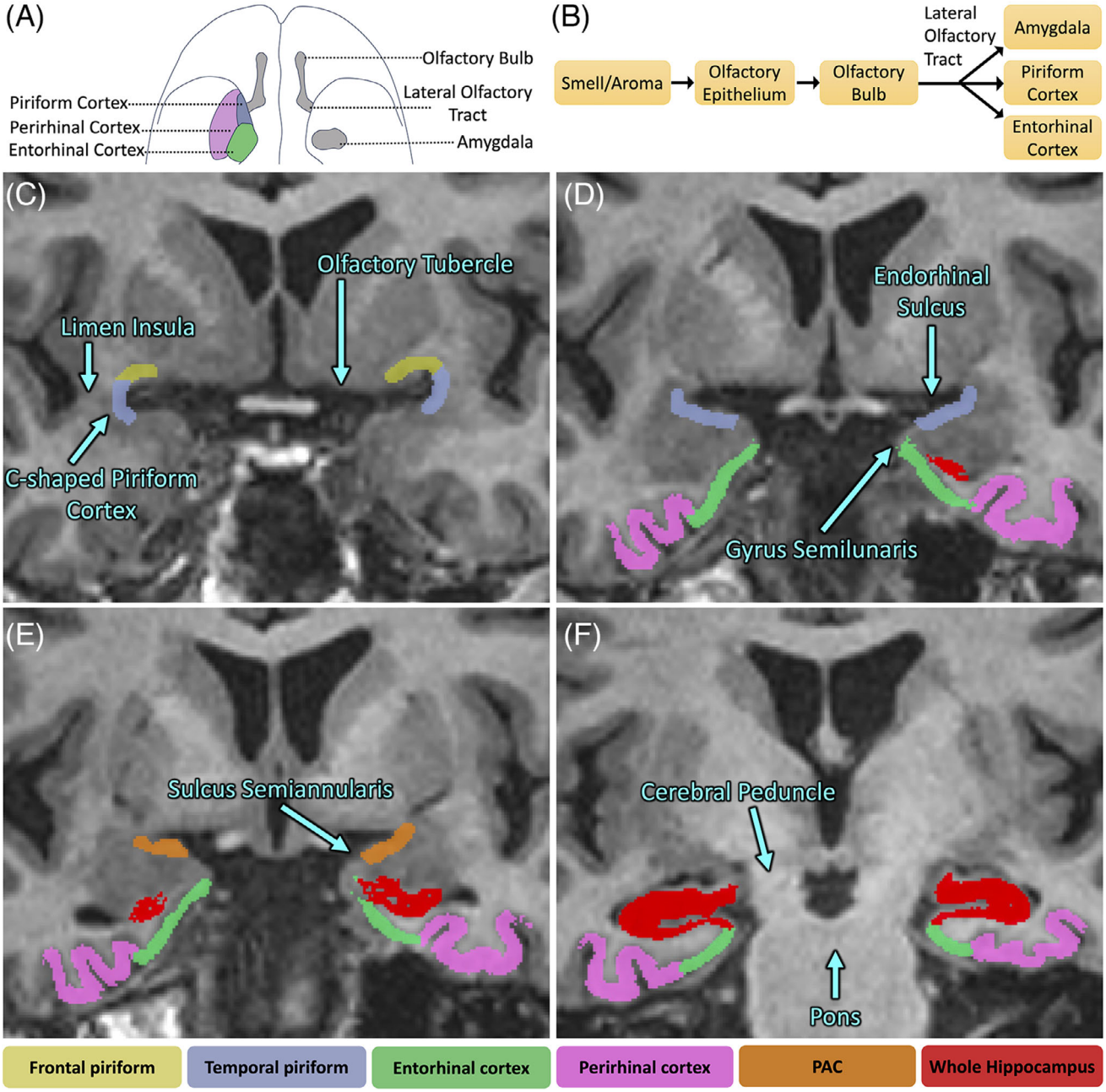

FIGURE 1 Piriform segmentation procedure overlaid on a T1-weighted three-dimensional (3D) inversion-recovery fast spoiled gradient echo (IR-FSPGR) image. (A) Inferior-perspective brain illustration depicting the location of the piriform cortex with respect to other regions of the olfactory circuit. (B) Schematic view of the olfactory circuit connections. (C) The first most anterior slice starts where the white matter of the limen insula is completely fused. Frontal piriform (PirF) and temporal piriform (PirT) are segmented, forming halves of a "C." PirF is segmented ~50% of the approximate distance to the olfactory tubercle, whereas PirT is segmented ~30% to the apex of the gyrus semilunaris. (D) PirF was not segmented. PirT was extended to 100% of the distance to the sulcus semiannularis. (E) PirT was replaced with periamygdaloid cortex (PAC), which was segmented the entire length of the gyrus semilunaris to the sulcus semiannularis. (F) Slice ~8: The appearance of the hippocampal fissure along the inferior aspect of the undulations of the hippocampal head marked the end of periamygdaloid segmentation. Note that the amygdala is segmented separately.

to participant diagnosis (HMT). Two additional individuals (EVS, SL) similarly quality-checked all the participants' segmentations and confirmed the coregistration of the T1w and T2w scans and segmentations.

2.7 | Regional data analysis

The PET image was resampled into T2 space using a single affine transformation derived from the T1-T2 co-registration above. Mean

PET standardized uptake value (SUV) was averaged for each region of interest (ROI) and across hemispheres. SUV ratio (SUVr) was computed using inferior cerebellar gray matter as the reference region.[22] Regional volumes were all corrected by partialling out total intracranial volume (ICV)[35] as measured by FreeSurfer.

2.8 | Behavioral assessments

AD, MCI, the ADRC healthy controls, and PD-CU (cognitively unimpaired) participants with available neuropsychology scores included four neuropsychological memory tests: the Craft Story delayed recall, Hopkins Verbal Learning Test – Revised (HVLT-R) delayed recall, Benson figure delayed recall, and Free and Cued Selective Reminding Test (FCSRT) delayed free recall. Individual scores were first z-scored in reference to baseline visits from 236 CU ADRC participants, and the four z-scores were then averaged to create a memory composite score.

The SAMS HCs completed three memory tests [i.e., Wechsler Memory Scale 3rd Edition Logical Memory (WMS-III LM), HVLT-R, and Brief Visuospatial Memory Test—Revised (BVMT-R)] and delayed recall. Scores were first z-scored in reference to the full SAMS sample and the three z-scores were then averaged to create a memory composite for each participant.[36] Given the differences in the underlying measures, the ADRC and SAMS memory composites were not combined.

Only cognitive scores within 3 years of the tau PET scan were considered.

Measures of olfactory function were unavailable for this cohort.

2.9 | Statistics

Demographic variables were compared across cohorts using a Kruskal-Wallis test and Fisher's exact tests.

We hypothesized increasing regional tau uptake among the four ordinal participant categories along the AD spectrum (amyloid–HC, amyloid+HC, MCI, AD). Distributions appeared non-normal, so we assessed for ordinal increase in tau uptake (and decrease in ICV-corrected volumes) across four regions bilaterally (entorhinal-perirhinal, piriform cortex, amygdala, and whole hippocampus = CA1-4 + DG + subiculum) using a nonparametric Jonckheere-Terpstra test in Stata 15 with one-sided uncorrected *p*-values reported.

Similar tests were performed on tau uptake on a control region, the precentral gyrus as segmented by FreeSurfer.

All cohort comparisons (e.g., between amyloid–HC and amyloid+HC, or amyloid–HC and PD-CU) were performed using a two-sided Wilcoxon rank-sum test.

With use of a Spearman's rank correlation after partialling out effects of age and sex, tau was correlated with a memory composite score for the full ADRC cohort ($n = 42/58$ scores available since $n = 2$ were excluded due to cognitive scores >3 years of tau PET scan, and $n = 14$ did not have memory composite scores available) and a memory composite score for the SAMS cohort ($n = 35/38$ scores available as $n = 3$ were excluded due to cognitive scores >3 years of tau PET scan).

Reported *p*-values are uncorrected.

3 | RESULTS

3.1 | Demographics

The mean age, mean years of education, and sex did not differ significantly between groups ($p = 0.313$, $p = 0.097$, and $p = 0.290$, respectively; Table 1). Approximately 88%, 40%, and 50% of MCI, HC, and PD-CU were amyloid positive, respectively. Participants were 94% non-Hispanic and 84% White.

3.2 | Volume

Regional volume adjusting for total intracranial volume was inversely correlated with AD spectrum disease severity, such that AD had the lowest volume followed by MCI, amyloid+HC, and amyloid–HC in the following regions (Figure 2): entorhinal-perirhinal ($J^* = 4.068$, $p < 0.001$), piriform-PAC ($J^* = 2.146$, $p = 0.016$), amygdala ($J^* = 5.276$, $p < 0.001$), and whole hippocampus ($J^* = 4.782$, $p < 0.001$). Amyloid+HC had lower volume than amyloid–HC in amygdala ($z = 2.733$, $p = 0.006$, Figure 2C), but not in entorhinal-perirhinal ($z = 0.537$, $p = 0.591$), piriform-PAC ($z = 0.764$, $p = 0.445$), or whole hippocampus ($z = 1.513$, $p = 0.130$). There was a statistically significant difference in volume between PD-CU and amyloid–HC only in the piriform-PAC ($z = 2.041$, $p = 0.041$, lower in PD-CU, Figure 2B) and not significant in entorhinal-perirhinal ($z = 0.023$, $p = 0.982$), amygdala ($z = 0.907$, $p = 0.364$), and whole hippocampus ($z = 0.907$, $p = 0.364$). Further evaluation of the same PD-CU and amyloid–HC difference within the piriform-PAC subregions shows localization to the frontal but not temporal or periamygdaloid portions of the piriform cortex (frontal piriform: $z = 3.312$, $p < 0.001$; temporal piriform: $z = 0.975$, $p = 0.329$; periamygdaloid: $z = 1.678$, $p = 0.093$). Volume was correlated between subregions, although less so with the piriform-PAC (Table S1). Across the entire cohort, volume was significantly different between sexes in the piriform-PAC (female median 720 mm^3, male 777 mm^3, $z = -2.220$, $p = 0.026$), but not in entorhinal-perirhinal ($z = -0.581$, $p = 0.562$), amygdala ($z = -1.878$, $p = 0.060$), or whole hippocampus ($z = -0.406$, $p = 0.685$). Age was negatively correlated with volume in the entorhinal-perirhinal cortex (Spearman's $\rho = -0.264$, $p = 0.010$) and whole hippocampus (Spearman's $\rho = -0.250$, $p = 0.015$), but not piriform-PAC or amygdala ($p > 0.05$, Table S2).

3.3 | Tau SUVr

Regional tau uptake was highest in AD followed by MCI, amyloid+HC, and amyloid–HC, in all four regions (Figure 3): entorhinal-perirhinal ($J^* = -6.157$, $p < 0.001$), piriform-PAC ($J^* = -5.646$, $p < 0.001$), amygdala ($J^* = -4.817$, $p < 0.001$), and whole hippocampus ($J^* = -3.989$, $p < 0.001$). Amyloid+HC had more tau than amyloid–HC in entorhinal-perirhinal ($z = -2.245$, $p = 0.025$) and piriform-PAC ($z = -2.033$, $p = 0.042$), but not in amygdala ($z = -1.334$, $p = 0.182$) or whole hippocampus ($z = -0.211$, $p = 0.833$). Separate examination of temporal, frontal, and periamygdaloid portions of piriform-PAC showed

TABLE 1 Demographics of the cohort in our study.

	AD	MCI	Healthy control (HC)	Parkinson's disease, cognitively unimpaired (PD-CU)	*p*-value
Age	71.25 ± 7.99	69.28 ± 13.72	71.72 ± 7.69	72.51 ± 6.12	0.313
Years of education*	17.67 ± 2.45	16.25 ± 1.98	17.09 ± 2.05	16.64 ± 1.86	0.097
Sex (M/F)	7/8	5/3	22/35	9/5	0.290
Amyloid ±	15/0	7/1	23/34	7/7	<0.001
Total N	15	8	57	14	

*Years of education were available for 9/8/57/14 AD/MCI/HC/PD-CU participants.

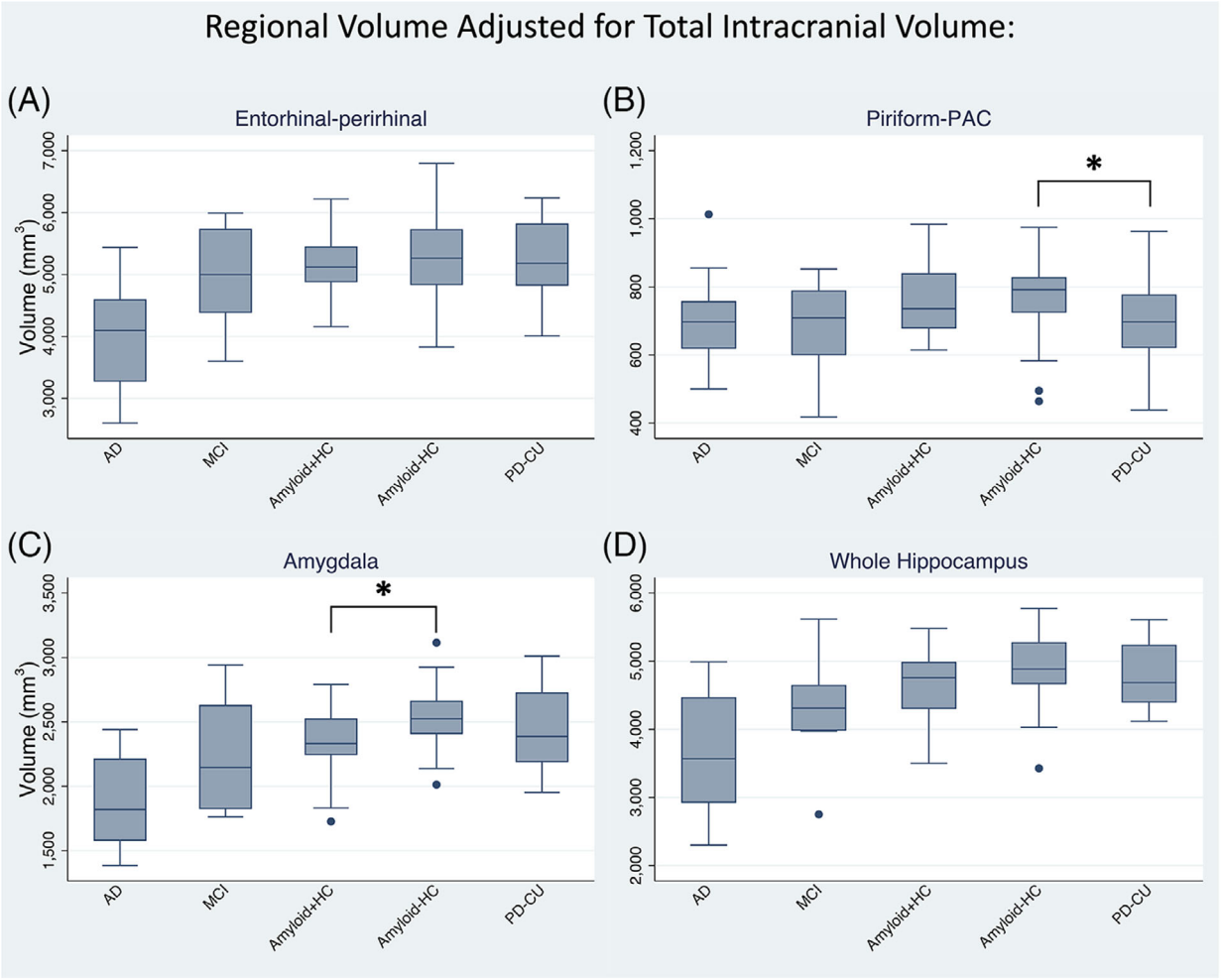

FIGURE 2 Regional volume corrected for total intracranial volume in Alzheimer's disease (AD), mild cognitive impairment (MCI), amyloid-positive/-negative healthy controls (amyloid+HC/amyloid−HC), and cognitively unimpaired Parkinson's disease (PD-CU). (A) Entorhinal-perirhinal, (B) Piriform-PAC (periamygdaloid cortex), (C) amygdala, and (D) whole hippocampus volumes. All show cross-sectionally increased volumes with decreasing disease status along the AD spectrum. * = Normal (cognitively unimpaired) PD-CU showed decreased piriform-PAC volume compared to amyloid−HC ($p = 0.041$), and amyloid+HC showed decreased amygdala volume compared to amyloid−HC ($p = 0.006$).

a similar gradation of tau uptake with disease severity (frontal: $J^* = -3.213$, $p < 0.001$; temporal: $J^* = -5.893$, $p < 0.001$; periamygdaloid: $J^* = -5.637$, $p < 0.001$, Figure S2), with the difference between amyloid+HC and amyloid−HC present in the temporal piriform and periamygdaloid cortex but not the frontal piriform (temporal: $z = -1.968$, $p = 0.049$; periamygdaloid: $z = -2.310$, $p = 0.021$; frontal: $z = 0.325$, $p = 0.745$). Separately comparing frontal versus temporal-piriform-PAC tau uptake across groups, showed a greater uptake for temporal-piriform-PAC than frontal piriform in AD ($z = 3.067$, $p = 0.002$), less uptake in amyloid−HC ($z = -4.112$, $p < 0.001$) and

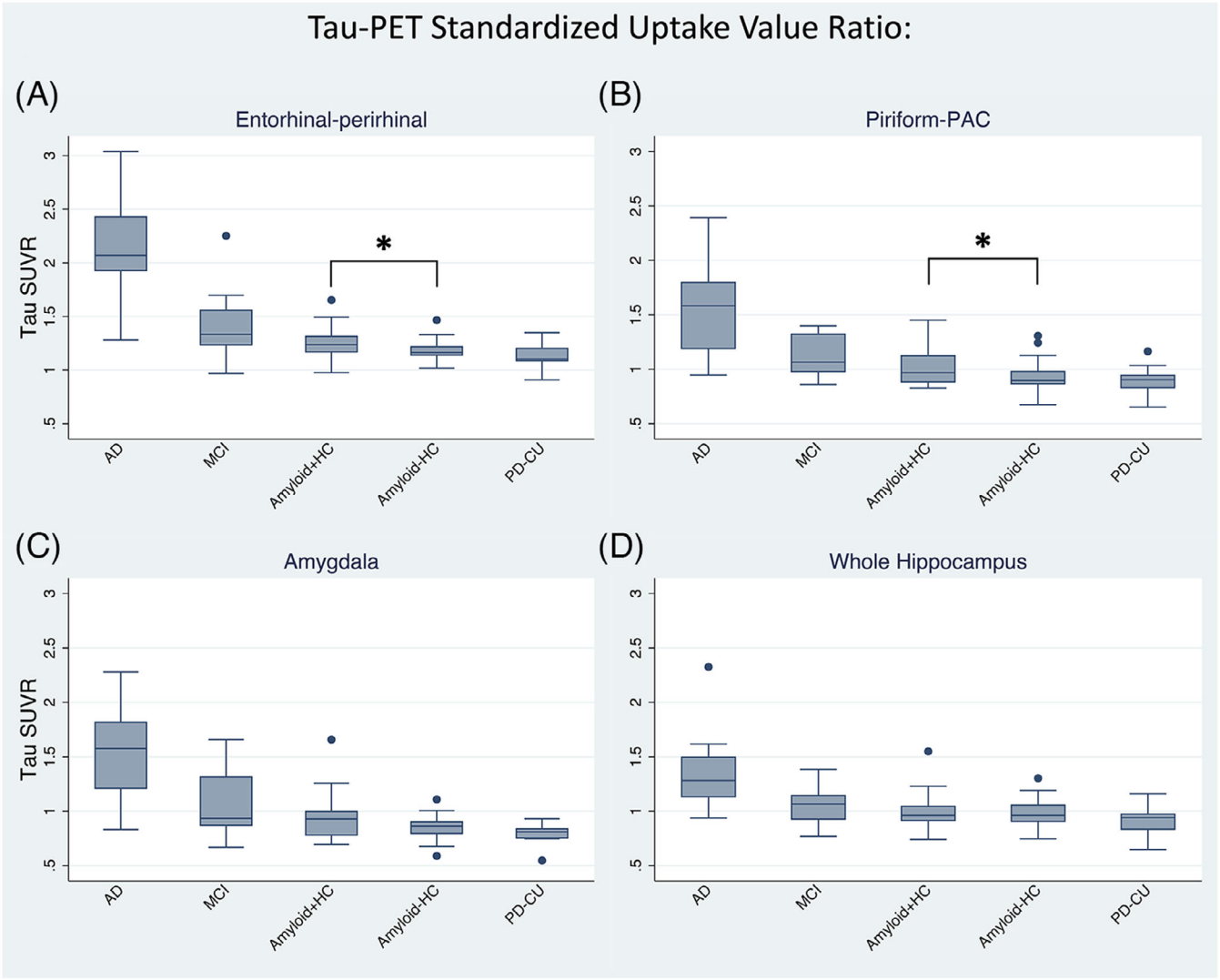

FIGURE 3 ^{18}F-PI-2620 tau uptake referenced to the inferior cerebellum. (A) Entorhinal-perirhinal volume, (B) piriform-PAC (periamygdaloid cortex), (C) amygdala, and (D) whole hippocampus. All show cross-sectionally increased tau with increasing disease status. * = Amyloid+HC showed increased tau uptake compared to amyloid−HC in entorhinal-perirhinal ($p = 0.025$) and piriform-PAC ($p = 0.042$).

PD-CU ($z = -2.229$, $p = 0.026$), and statistically equivalent in MCI ($z = -0.140$, $p = 0.887$) and amyloid+HC ($z = -0.152$, $p = 0.879$). To evaluate tau levels across regions within amyloid-negative healthy older adults, we compared exclusively amyloid−HC and found higher tau SUVr in entorhinal-perirhinal compared to piriform-PAC, amygdala, and whole hippocampus ($p < 0.001$). Uptake of tau was significantly correlated between these adjacent subregions (Table S3), and uptake did not differ between sexes ($p > 0.05$) and did not show a correlation with age in any subregion ($p > 0.05$).

Uptake of tau was not elevated in any of these regions in PD-CU (Figure 3), with statistical equivalence to amyloid−HC in the entorhinal-perirhinal ($z = 1.179$, $p = 0.238$), piriform-PAC ($z = 0.658$, $p = 0.511$), amygdala ($z = 1.633$, $p = 0.102$), and whole hippocampus ($z = 1.066$, $p = 0.286$).

Comparing tau with the precentral gyrus reference region (generally involved in late AD) showed a similar ordinal gradation of tau uptake ($J^* = -2.719$, $p = 0.003$) (Figure S3). If the AD category was excluded, no significant ordinal gradation existed between precentral tau uptake across MCI, amyloid+HC, and amyloid−HC ($J^* = -0.946$, $p = 0.172$), whereas piriform-PAC still showed a significant ordinal gradation when excluding AD ($J^* = -2.989$, $p = 0.001$).

3.4 | Behavior relationships of tau-memory

The memory composite scores in the ADRC cohort ($n = 42$ available) showed a negative monotonic relationship with tau uptake in all four regions (Figures 4 & S4): entorhinal-perirhinal (Spearman's $\rho = -0.516$, $p < 0.001$), piriform-PAC (Spearman's $\rho = -0.543$, $p < 0.001$), amygdala (Spearman's $\rho = -0.587$, $p < 0.001$), and whole hippocampus (Spearman's $\rho = -0.531$, $p < 0.001$). Within the piriform-PAC subregions, this negative relationship was present in frontal piriform (Spearman's

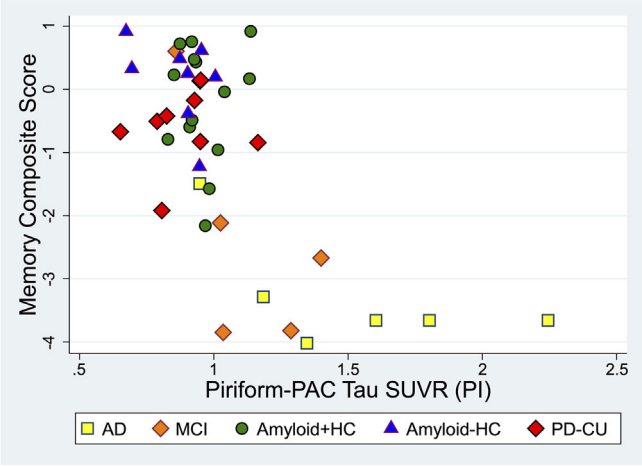

FIGURE 4 Alzheimer's Disease Research Center (ADRC) behavioral correlations with piriform-PAC (periamygdaloid cortex) tau uptake. The memory composite score displayed a negative monotonic relationship relative to tau uptake in all four regions across participants, with piriform-PAC tau shown here, and other regions in Figure S4.

$\rho = -0.325$, $p = 0.036$), temporal piriform (Spearman's $\rho = -0.534$, $p < 0.001$), and periamygdaloid cortex (Spearman's $\rho = -0.552$, $p < 0.001$). Among the smaller subsample of amyloid+HC ($n = 14$) and amyloid−HC ($n = 8$) in the ADRC cohort, the memory composite score did not show a significant negative correlation ($p > 0.05$) in any of the four regions.

The memory composite in the full SAMS cohort (which are all amyloid+HC and amyloid−HC, $n = 35$) did not show a significant relationship relative to tau uptake across the four regions ($p > 0.05$). The memory composite of amyloid+HC controls showed a significant negative monotonic relationship in the piriform-PAC (Spearman's $\rho = -0.738$, $p = 0.037$, Figure S5), which localized to temporal piriform and periamygdaloid cortex: (frontal piriform: Spearman's $\rho = -0.595$, $p = 0.120$; temporal piriform: Spearman's $\rho = -0.810$, $p = 0.015$; periamygdaloid cortex; Spearman's $\rho = -0.738$, $p = 0.037$), whereas no other regions showed a significant relationship for amyloid+HC or amyloid−HC separately ($p > 0.05$).

4 | DISCUSSION

4.1 | Key findings

Uptake of tau increased cross-sectionally with disease severity across all four regions examined (entorhinal-perirhinal; the frontal, temporal, and periamygdaloid portions of the piriform-PAC; amygdala; and whole hippocampus). AD participants showed the highest tau uptake, followed by MCI, amyloid+HC, and lastly amyloid−HC. In addition, we found significantly higher uptake in the amyloid+HC cohort compared to the amyloid−HC group in the entorhinal-perirhinal cortices and piriform-PAC, but not in the amygdala or whole hippocampus. Comparison with cognitive testing, specifically episodic memory performance, across the whole cohort showed worse memory scores with increasing tau in the piriform-PAC. Finally, PD-CU did not show elevated tau uptake and instead showed piriform-PAC atrophy, specifically involving the frontal piriform cortex.

4.2 | Pathological and clinical correlations

The expected progression of supratentorial tau in AD is thought to begin in the transentorhinal cortex and spread to adjacent cortices.[37] More recently, direct neuropathological evaluation of the piriform cortex with respect to its three-layer allocortical architecture has revealed senile amyloid plaques surrounded by neurofibrillary tangles, primarily in the superficial aspect of layer II, accompanied by differential interneuron vulnerability.[18] Supporting the known pathological appearance of piriform tau in AD, we found increasing tau uptake cross-sectionally in our study. The uptake was stronger in the temporal compared to the frontal piriform in AD, which could relate to possible closer synaptic proximity to the transentorhinal region; in fact, all the significant tau findings for piriform-PAC were also significant for the temporal piriform. We further found that only piriform-PAC and entorhinal-perirhinal tau were statistically different between amyloid+ and amyloid− healthy controls, suggesting that piriform tau uptake is an early event in AD. The correlation of piriform uptake with memory performance could relate to the close connectivity of olfactory circuitry with the entorhinal cortex.

Neurofibrillary pathology has also been found in areas preceding the piriform cortex in the olfactory circuit (Figure 1B), such as the olfactory bulb, tract, and the anterior olfactory nucleus.[19] Early olfactory deficits in AD[38–40] may be influenced by the entirety of the olfactory circuit, including the piriform neurofibrillary pathology we are measuring with tau PET-MR. There was a relative lack of piriform-PAC (or any medial temporal) tau uptake in PD-CU. This finding is consistent with PD post-mortem data, where the olfactory bulb has shown notable neurodegeneration and presence of Lewy bodies,[41,42] which points to the source of hyposmia in PD being primarily linked to olfactory bulb degeneration and not the piriform cortex. The volume loss we observe in the piriform cortex in PD may thus be secondary to α-synuclein pathology[43,44] in the upstream olfactory bulb.

4.3 | Comparisons with other imaging studies

Task-based functional MRI activation of the piriform cortex during olfaction has shown blunted response not only in AD[45] but also MCI.[46] Microstructural connectivity, as measured by diffusion tensor imaging graph theory metrics, has enabled classification of disease status based on piriform connectivity.[47] Our work reveals tau deposition in the piriform-PAC in early AD that could drive neurodegeneration and dysfunction, and thus explain differences in functional and diffusion imaging. A decrease in piriform cortex volume in a larger cohort of AD/MCI has been identified in prior work,[30] whereas the differences in tau PET reported here are revealed in a smaller cohort, suggesting that

molecular specificity offers improved detection of disease-relevant pathology.

4.4 | Limitations

We utilized manual frontal piriform, temporal piriform, and periamygdaloid cortex segmentation, with all steps done blind to diagnosis. Future work can explore newly-available automated segmentation.[30] The piriform-PAC is small and adjacent to other structures with tau burden in AD (e.g., the amygdala),[26] with some uncertainty in boundaries between its internal components. Nevertheless, we see differences in tau effects between piriform-PAC and amygdala, arguing that they reflect separate measurements. In addition, ongoing work with PET-MR can potentially improve acquired and reconstructed PET resolution.[48] Our sample size can limit subgroup analyses, although we still are able to detect not only ordinal differences but also discriminate amyloid+ versus amyloid− controls. Future work can integrate shared data sets of tau PET scans to further increase power, although segmentation strategy may change and be based solely on T1-weighted images. Our cross-sectional study provides a single-timepoint snapshot of the groups studied, so future longitudinal studies should inform on the dynamics of tau progression in the piriform cortex compared to the adjacent medial temporal structures. Future work will complement this with other tracers, including synaptic tracers, fluorodeoxyglucose (FDG), and amyloid. Study participants were predominantly non-Hispanic White, and future studies will specifically enroll more diverse populations. Finally, olfactory discrimination is not routinely assessed in AD studies or in our presented work. Especially with coronavirus disease 2019 (COVID-19), established olfactory assessment is increasingly practical[49,50] and will be pursued with ongoing work.

5 | CONCLUSIONS

We show significant cross-sectional differences in the olfactory and memory circuits noninvasively with tau PET-MR, with early cross-sectional elevation in piriform-PAC tau uptake closely tracking adjacent medial temporal regions in AD but not in cognitively unimpaired PD. Deposition of tau may potentially track or even explain olfactory dysfunction in AD and should be the subject of future investigations.

ACKNOWLEDGMENTS

This study was funded by the National Institutes of Health (NIH) (Stanford Alzheimer's Disease Research Center (ADRC) P30AG066515, P50AG047366, R21AG058859, R01AG048076, R01AG074339, R01AG061120, K99AG071837, R01NS115114), the Alzheimer's Association (AARFD-21-849349), the Good Planet Foundation, the Stanford Wu Tsai Neurosciences Institute, and the Stanford Precision Health and Integrated Diagnostics (PHIND) Center.

CONFLICT OF INTEREST STATEMENT

Dr Kathleen Poston has been funded by grants to conduct research from the Michael J Fox Foundation for Parkinson's Research, the Knight Initiative for Brain Resilience, the Wu Tsai Neurosciences Institute, the Lewy Body Dementia Association, the Alzheimer's Drug Discovery Foundation, the Sue Berghoff LBD Research Fellowship, and the National Institutes of Health (NIH). She is on the Scientific Advisory Board for Curasen where she receives consulting fees and stock options. She is on the Scientific Advisory Board for Amprion, where she receives stock options. She is a consultant for Novartis, Biohaven, and Neuron23, where she receives consulting fees. Dr Michael Zeineh receives research funding from GE Healthcare. All other authors have no disclosures relevant to this manuscript. Author disclosures are available in the Supporting Information.

CONSENT STATEMENT

All participants provided written informed consent in accordance with HIPAA and the Stanford Institutional Review Board.

ORCID

Hossein Moein Taghavi https://orcid.org/0000-0002-8585-1634

REFERENCES

1. Braak H, Alafuzoff I, Arzberger T, Kretzschmar H, Tredici K. Staging of Alzheimer disease-associated neurofibrillary pathology using paraffin sections and immunocytochemistry. *Acta Neuropathol*. 2006;112(4):389-404. doi:10.1007/S00401-006-0127-Z/FIGURES/5
2. Gallardo G, Holtzman DM. Amyloid-β and Tau at the Crossroads of Alzheimer's Disease. *Adv Exp Med Biol*. 2019;1184:187-203. doi:10.1007/978-981-32-9358-8_16/FIGURES/1
3. Soria Lopez JA, González HM, Léger GC. Chapter 13 - Alzheimer's disease. In: Dekosky ST, Asthana S, eds. *Handbook of Clinical Neurology*. Geriatric Neurology. Elsevier; 2019:231-255. doi:10.1016/B978-0-12-804766-8.00013-3
4. Doty RL. *Handbook of Olfaction and Gustation*. 3rd ed. 2015:1-1264. doi:10.1002/9781118971758. Published online June.
5. Tian Q, Bilgel M, Moghekar AR, Ferrucci L, Resnick SM. Olfaction, Cognitive Impairment, and PET Biomarkers in Community-Dwelling Older Adults. *J Alzheimers Dis : JAD*. 2022;86(3):1275-1285. doi:10.3233/JAD-210636
6. Misiak MM, Hipolito MS, Ressom HW, Obisesan TO, Manaye KF, Nwulia EA. Apo E4 Alleles and Impaired Olfaction as Predictors of Alzheimer's Disease. *Clin Exp Psychol*. 2017;3(4):169. doi:10.4172/2471-2701.1000169
7. Goodsmith MS, Wroblewski KE, Schumm LP, Ma MK, Mcclintock JM, Pinto N®. Association of APOE ε4 Status with Long-term Declines in Odor Sensitivity, Odor Identification, and Cognition in Older US Adults. *Neurology*. 2023;101(13):e1341-e1350. doi:10.1212/WNL.0000000000207659
8. Audronyte E, Pakulaite-Kazliene G, Sutnikiene V, Kaubrys G. Odor Discrimination as a Marker of Early Alzheimer's Disease. *J Alzheimers Dis*. 2023;94(3):1169. doi:10.3233/JAD-230077
9. van Hartevelt TJ, Kringelbach ML. The Olfactory System. *The Human Nervous System*. 3rd ed. 2012:1219-1238. doi:10.1016/B978-0-12-374236-0.10034-3. Published online January.
10. Majak K, Rönkkö S, Kemppainen S, Pitkänen A. Projections from the amygdaloid complex to the piriform cortex: a PHA-L study in the rat. *J Comp Neurol*. 2004;476(4):414-428. doi:10.1002/cne.20233

11. Hummel T, Whitcroft KL, Andrews P, et al. Position paper on olfactory dysfunction. *Rhinol Suppl*. 2017;54(26):1-30. doi:10.4193/Rhino16.248
12. Wilson RS, Schneider JA, Arnold SE, Tang Y, Boyle PA, Bennett DA. Olfactory Identification and Incidence of Mild Cognitive Impairment in Older Age. *Arch Gen Psychiatry*. 2007;64(7):802-808. doi:10.1001/ARCHPSYC.64.7.802
13. Wilson RS, Arnold SE, Schneider JA, Boyle PA, Buchman AS, Bennett DA. Olfactory Impairment in Presymptomatic Alzheimer's Disease. *Ann NY Acad Sci*. 2009;1170(1):730-735. doi:10.1111/J.1749-6632.2009.04013.X
14. Rajani V, Yuan Q. Noradrenergic Modulation of the Piriform Cortex: a Possible Avenue for Understanding Pre-Clinical Alzheimer's Disease Pathogenesis. *Frontiers in Cellular Neuroscience*. 2022;16:908758. doi:10.3389/fncel.2022.908758
15. Ponsen MM, Stoffers D, Booij J, Eck-Smit BLFV, Wolters EC, Berendse HW. Idiopathic hyposmia as a preclinical sign of Parkinson's disease. *Ann Neurol*. 2004;56(2):173-181. doi:10.1002/ANA.20160
16. Boesveldt S, Verbaan D, Knol DL, et al. A comparative study of odor identification and odor discrimination deficits in Parkinson's disease. *Movement Disorders : Official Journal of the Movement Disorder Society*. 2008;23(14):1984-1990. doi:10.1002/MDS.22155
17. He R, Zhao Y, He Y, et al. Olfactory Dysfunction Predicts Disease Progression in Parkinson's Disease: a Longitudinal Study. *Front Neurosci*. 2020;14. doi:10.3389/FNINS.2020.569777
18. Saiz-Sanchez D, De la Rosa-Prieto C, Ubeda-Banon I, Martinez-Marcos A. Interneurons, tau and amyloid-β in the piriform cortex in Alzheimer's disease. *Brain Struct Funct*. 2015;220(4):2011-2025. doi:10.1007/S00429-014-0771-3/FIGURES/9
19. Kroth H, Oden F, Molette J, et al. Discovery and preclinical characterization of [18F]PI-2620, a next-generation tau PET tracer for the assessment of tau pathology in Alzheimer's disease and other tauopathies. *Eur J Nucl Med Mol Imaging*. 2019;46(10):2178-2189. doi:10.1007/S00259-019-04397-2/FIGURES/5
20. Mormino EC, Toueg TN, Azevedo C, et al. Tau PET imaging with 18F-PI-2620 in aging and neurodegenerative diseases. *Eur J Nucl Med Mol Imaging*. 2021;48(7):2233. doi:10.1007/S00259-020-04923-7
21. Mueller A, Bullich S, Barret O, et al. Tau PET imaging with 18F-PI-2620 in Patients with Alzheimer Disease and Healthy Controls: a First-in-Humans Study. *J Nucl Med*. 2020;61(6):911-919. doi:10.2967/JNUMED.119.236224
22. Carlson ML, Toueg TN, Khalighi MM, et al. Hippocampal subfield imaging and fractional anisotropy show parallel changes in Alzheimer's disease tau progression using simultaneous tau-PET/MRI at 3T. *Alzheimer's & Dementia: Diagnosis, Assessment & Disease Monitoring*. 2021;13(1):e12218. doi:10.1002/DAD2.12218
23. Gibb WRG, Lees AJ. The relevance of the Lewy body to the pathogenesis of idiopathic Parkinson's disease. *J Neurol Neurosurg Psychiatry*. 1988;51(6):745-752. doi:10.1136/JNNP.51.6.745
24. Pontecorvo MJ, Devous MD, Kennedy I, et al. A multicentre longitudinal study of flortaucipir (18F) in normal ageing, mild cognitive impairment and Alzheimer's disease dementia. *Brain : a Journal of Neurology*. 2019;142(6):1723-1735. doi:10.1093/BRAIN/AWZ090
25. Modat M, Cash DM, Daga P, Winston GP, Duncan JS, Ourselin S. Global image registration using a symmetric block-matching approach. *J Med Imaging (Bellingham)*. 2014;1(2):024003. doi:10.1117/1.JMI.1.2.024003
26. Pereira PMG, Insausti R, Artacho-Pérula E, Salmenperä T, Kälviäinen R, Pitkänen A. MR Volumetric Analysis of The Piriform Cortex and Cortical Amygdala in Drug-Refractory Temporal Lobe Epilepsy. *AJNR: American Journal of Neuroradiology*. 2005;26(2):319.
27. Vaughan DN, Jackson GD. The Piriform Cortex and Human Focal Epilepsy. *Front Neurol*. 2014;5:259. doi:10.3389/fneur.2014.00259
28. Ding SL, Royall JJ, Sunkin SM, et al. Comprehensive cellular-resolution atlas of the adult human brain. *J Comp Neurol*. 2016;524(16):3127-3481. doi:10.1002/cne.24080
29. Galovic M, Baudracco I, Wright-Goff E, et al. Association of Piriform Cortex Resection With Surgical Outcomes in Patients With Temporal Lobe Epilepsy. *JAMA Neurol*. 2019;76(6):690-700. doi:10.1001/jamaneurol.2019.0204
30. Steinbart D, Yaakub SN, Steinbrenner M, et al. Automatic and manual segmentation of the piriform cortex: method development and validation in patients with temporal lobe epilepsy and Alzheimer's disease. *Hum Brain Mapp*. 2023;44(8):3196-3209. doi:10.1002/HBM.26274
31. Koepp MJ, Galovic M, Baudracco I, et al. Association of Piriform Cortex Resection With Surgical Outcomes in Patients With Temporal Lobe Epilepsy. *JAMA Neurol*. 2019;76(6):690-700. doi:10.1001/JAMANEUROL.2019.0204
32. Iqbal S, Leon-Rojas JE, Galovic M, et al. Volumetric analysis of the piriform cortex in temporal lobe epilepsy. *Epilepsy Res*. 2022;185:106971. doi:10.1016/J.EPLEPSYRES.2022.106971
33. Yushkevich PA, Piven J, Hazlett HC, et al. User-guided 3D active contour segmentation of anatomical structures: significantly improved efficiency and reliability. *Neuroimage*. 2006;31(3):1116-1128. doi:10.1016/J.NEUROIMAGE.2006.01.015
34. Saygin ZM, Kliemann D, Iglesias JE, et al. High-resolution magnetic resonance imaging reveals nuclei of the human amygdala: manual segmentation to automatic atlas. *Neuroimage*. 2017;155:370-382. doi:10.1016/J.NEUROIMAGE.2017.04.046
35. Voevodskaya O. The effects of intracranial volume adjustment approaches on multiple regional MRI volumes in healthy aging and Alzheimer's disease. *Front Aging Neurosci*. 2014;6(OCT):93610. doi:10.3389/FNAGI.2014.00264/BIBTEX
36. Trelle AN, Carr VA, Wilson EN, et al. Association of CSF Biomarkers With Hippocampal-Dependent Memory in Preclinical Alzheimer Disease. *Neurology*. 2021;96(10):E1470-E1481. doi:10.1212/WNL.0000000000011477
37. Braak H, Braak E. Neuropathological stageing of Alzheimer-related changes. *Acta Neuropathol*. 1991;82(4):239-259. doi:10.1007/BF00308809
38. Roberts RO, Christianson TJH, Kremers WK, et al. Association Between Olfactory Dysfunction and Amnestic Mild Cognitive Impairment and Alzheimer Disease Dementia. *JAMA Neurol*. 2016;73(1):93-101. doi:10.1001/JAMANEUROL.2015.2952
39. Woodward MR, Hafeez MU, Qi Q, et al. Odorant item specific olfactory identification deficit may differentiate Alzheimer's disease from aging. *The American Journal of Geriatric Psychiatry : Official Journal of the American Association for Geriatric Psychiatry*. 2018;26(8):835. doi:10.1016/J.JAGP.2018.02.008
40. Stamps JJ, Bartoshuk LM, Heilman KM. A brief olfactory test for Alzheimer's disease. *J Neurol Sci*. 2013;333(1-2):19-24. doi:10.1016/J.JNS.2013.06.033
41. Braak H, Del Tredici K, Bratzke H, Hamm-Clement J, Sandmann-Keil D, Rüb U. Staging of the intracerebral inclusion body pathology associated with idiopathic Parkinson's disease (preclinical and clinical stages). *J Neurol*. 2002;249(3):III/1-5. doi:10.1007/s00415-002-1301-4
42. Braak H, Tredici KD, Rüb U, de Vos RAI, Jansen Steur ENH, Braak E. Staging of brain pathology related to sporadic Parkinson's disease. *Neurobiol Aging*. 2003;24(2):197-211. doi:10.1016/S0197-4580(02)00065-9
43. Kulkarni AS, Cortijo MDM, Roberts ER, et al. Perturbation of in vivo neural activity following α-Synuclein seeding in the olfactory bulb. *Journal of Parkinson's disease*. 2020;10(4):1411. doi:10.3233/JPD-202241
44. Fullard ME, Morley JF, Duda JE. Olfactory Dysfunction as an Early Biomarker in Parkinson's Disease. *Neuroscience bulletin*. 2017;33(5):515-525. doi:10.1007/S12264-017-0170-X

45. Li W, Howard JD, Gottfried JA. Disruption of odour quality coding in piriform cortex mediates olfactory deficits in Alzheimer's disease. *Brain*. 2010;133(9):2714-2726. doi:10.1093/BRAIN/AWQ209
46. Vasavada MM, Martinez B, Wang J, et al. Central Olfactory Dysfunction in Alzheimer's Disease and Mild Cognitive Impairment: a Functional MRI Study. *J Alzheimers Dis*. 2017;59(1):359-368. doi:10.3233/JAD-170310
47. Ebadi A, da Rocha JLD, Nagaraju DB, et al. Ensemble Classification of Alzheimer's Disease and Mild Cognitive Impairment Based on Complex Graph Measures from Diffusion Tensor Images. *Front Neurosci*. 2017;11(FEB):56. doi:10.3389/FNINS.2017.00056
48. Schramm G, Rigie D, Vahle T, et al. Approximating anatomically-guided PET reconstruction in image space using a convolutional neural network. *Neuroimage*. 2021;224:117399. doi:10.1016/J.NEUROIMAGE.2020.117399
49. Chiu A, Fischbein N, Wintermark M, Zaharchuk G, Yun PT, Zeineh M. COVID-19-induced anosmia associated with olfactory bulb atrophy. *Neuroradiology*. 2021;63(1):147. doi:10.1007/S00234-020-02554-1
50. Brann DH, Tsukahara T, Weinreb C, et al. Non-neuronal expression of SARS-CoV-2 entry genes in the olfactory system suggests mechanisms underlying COVID-19-associated anosmia. *Sci Adv*. 2020;6(31):eabc5801. doi:10.1126/SCIADV.ABC5801

SUPPORTING INFORMATION

Additional supporting information can be found online in the Supporting Information section at the end of this article.

How to cite this article: Moein Taghavi H, Karimpoor M, van Staalduinen EK, et al. Elevated tau in the piriform cortex in Alzheimer's but not Parkinson's disease using PET-MR. *Alzheimer's Dement*. 2024;16:e70040. https://doi.org/10.1002/dad2.70040